Running title: Intracellular pathway of LDLR degradation

SUPPLEMENTAL FIGURES

Fig.S1. **Levels of PCSK9 in mouse hepatocytes and plasma.** Immunoprecipitation followed by Western blot analysis of mouse PCSK9 (25): (a) secreted from primary hepatocytes of KO and WT mice, as compared to immunoprecipitation of 100 nM pure human PCSK9, used in Figure 5. This reflects the fact that levels of secreted PCSK9 from primary hepatocytes in 48h are much lower than 5 μg (100 nM). (b) Circulating PCSK9 in the plasma of $Ldlr^{+/+}$ or $Ldlr^{-/-}$ mice (pool of 3 mice each). Note the presence of the Furin-cleaved form (mouse $PCSK9_{\Delta N221}$), and the much higher levels of PCSK9 in $Ldlr^{-/-}$ mouse plasma.

Fig. S2**. Raw data from FACS analyses of HepG2 cells overexpressing PCSK9.** As described in Figure 1, HepG2 cells were transiently transfected with the non-secreted inactive site mutant (pIR-PCSK9-H226A), pIR-PCSK9-WT or the gain of function mutant (pIR-PCSK9-D374Y). 24h post-transfection, cells were sorted both for EGFP (PCSK9-expressing cells; GFP+/-) and cell surface LDLR. The plots are representative of three separate experiments. To evaluate the loss of cell surface LDLR, $LDLR^-$ events were divided by the total of the corresponding GFP areas (GFP^+ or GFP^-). As reported (5), overexpression of catalytically inactive PCSK9 (pIR-PCSK9-H226A) is not secreted and was used for normalization. The data are representative of 3 separate experiments.

Fig. S3. **Overexpression of PCSK9 in HEK293 cells did not affect cell surface LDLR on adjacent, un-transfected cells.** HEK293 cells were transiently transfected with pIR-PCSK9-WT. At 24h post-transfection, different ratios (panels 1-5) of non-transfected and PCSK9-transfected cells were mixed, keeping a total of $1x10^6$ cells. (a) For each ratio, cells were sorted using a fixed gating of 10^4 events of naive cells (GFP^-). (b) For each condition are represented: the % of transfected and non-transfected cells, concentration (nM) of secreted PCSK9, and % of LDLR-negative cells among GFP^+ or GFP^- cells. This is a representative experiment of 2 separate ones.

Fig. S4. **KD_{CLCs} in HepG2 cells increase LDLR levels without inhibition of LDLR endocytosis.** (a) 72h post-transfection, Permeabilized HepG2 cells were stained with antibodies to clathrin light chains (CLC; red) or LDLR (green). Arrows point to the cell surface and perinuclear region. This is a representative experiment of 2 separate ones. [**b**] HepG2 cells were transiently transfected with either a non-silencing siCtl or with siCLCa+b. At 72h post-transfection, cells were incubated for 2h with 4 μg/ml of diI-LDL. Immunocytochemistry revealed that upon KD_{CLCs} (green), LDL endocytosis was increased, as illustrated by intracellular uptake of diI-LDL (red). This is a representative experiment of 3 separate ones. Scale bars = 20 μm.

Fig. S5. ***De novo* biosynthesis of LDLR upon KD_{CLCs}.** HepG2 cells were transiently transfected with either a non-silencing siRNA (siCtl) or with siRNAs against both clathrin light chain (CLC) a and b isoforms (siCLCa+b). At 72h post-transfection, non-transfected HepG2 cells (mock) or transfected cells were washed 2x with DMEM media and incubated for 4h with ^{35}S-Met/Cys. Then, LDLR was immunoprecipitated and analyzed by autoradiography. Quantitation of the ~160 kDa mature LDLR is emphasized. These data are representative of 2 independent experiments.

Fig.S6. **Western blotting of selected stable pools of shRNA-expressing HepG2 cells.** Analysis of 1 or 2 cellular pools expressing no shRNA (pLKO, empty vector), shNT (non-target shRNA) or two different shRNAs against PCSK9 (shPCSK9-1 or 2). For most shRNA constructs, two separate pools were generated (a or b). The comparative analysis of LDLR, PCSK9 (normalized to β-actin), and transferrin receptor (TfR) are shown.

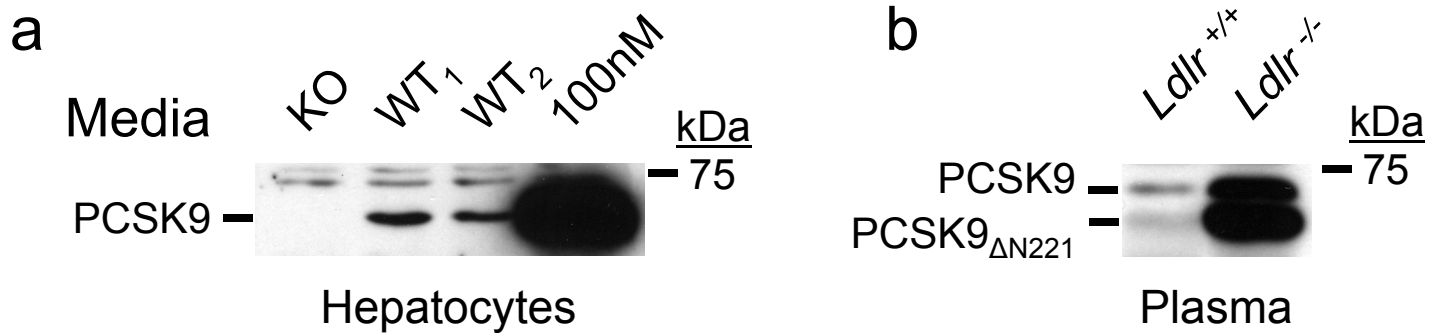
a
Media
KO
WT1
WT2
100nM
kDa
75
PCSK9
Hepatocytes
b
Ldlr+/+
Ldlr-/-
kDa
75
PCSK9
PCSK9ΔN221
Plasma

Fig.S1

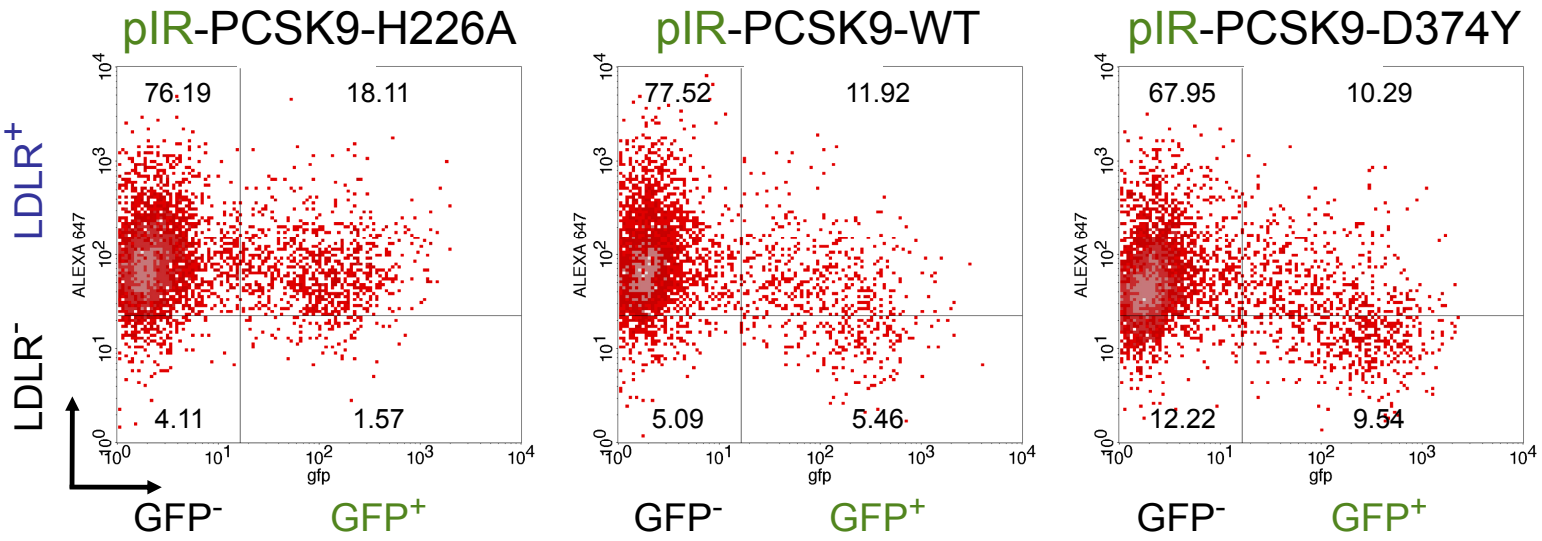
pIR-PCSK9-H226A
pIR-PCSK9-WT
pIR-PCSK9-D374Y
LDLR+
LDLR-
GFP-
GFP+
ALEXA 647
gfp
76.19
18.11
4.11
1.57
77.52
11.92
5.09
5.46
67.95
10.29
12.22
9.54

Fig.S2

a

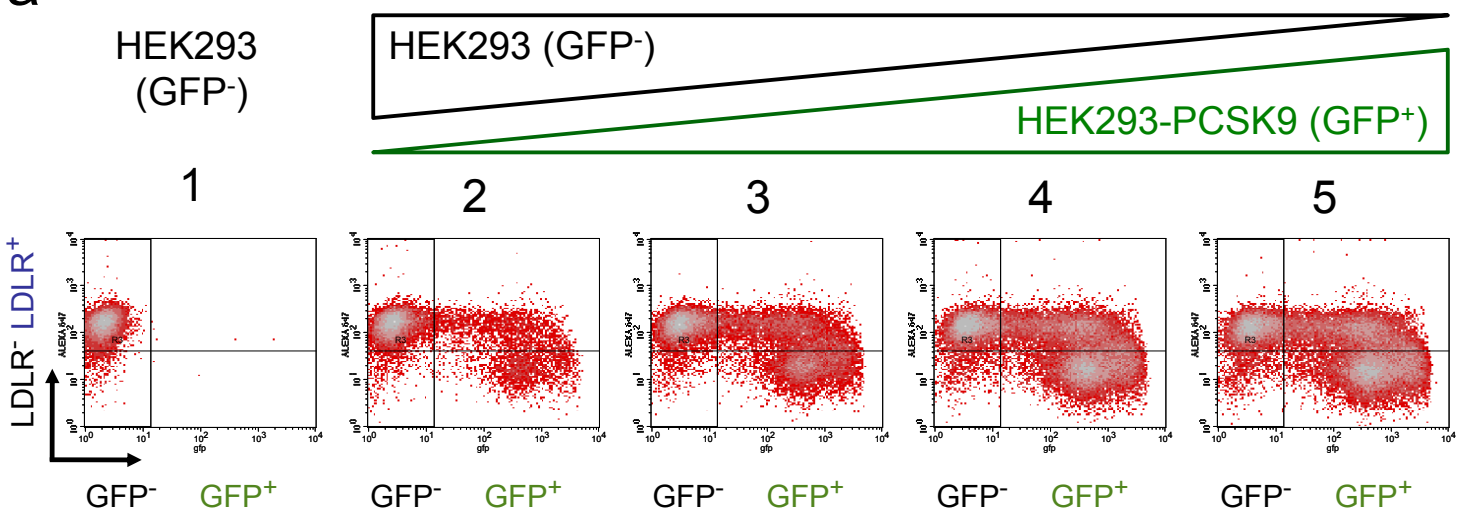

b

	1	2	3	4	5
HEK293 (GFP-; %)	100.0	66.8	41.5	29.8	27.1
HEK293-PCSK9 (GFP+; %)	0.0	33.1	58.5	70.2	72.9
PCSK9 (media; nM)	0.0	7.2	15.1	19.0	20.6
GFP+ (LDLR-negative; %)	N/A	45.0	46.4	53.3	57.3
GFP- (LDLR-negative; %)	**3.4**	**4.4**	**5.2**	**7.4**	**9.8**

Fig.S3

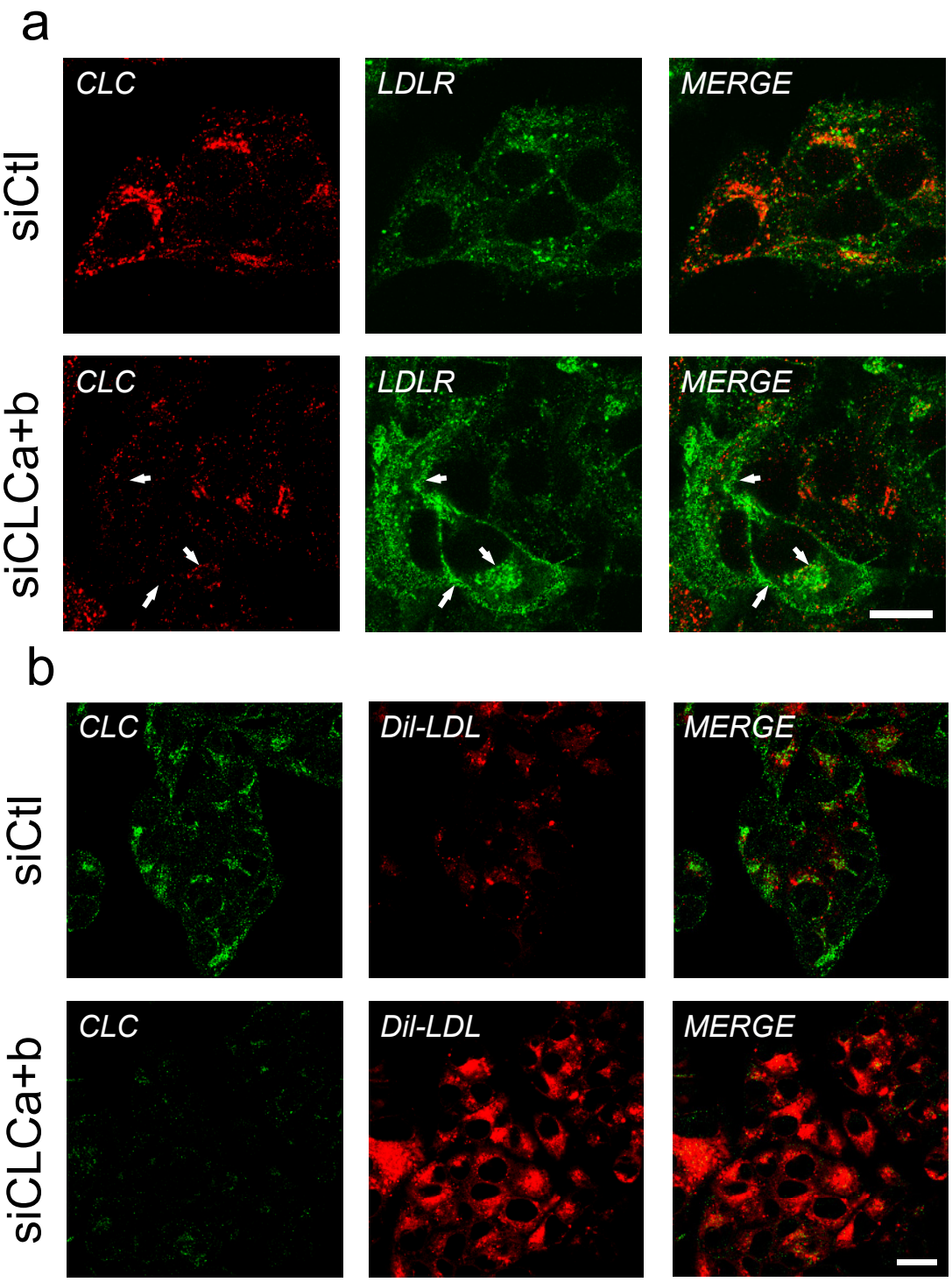
a
siCtl
CLC
LDLR
MERGE
siCLCa+b
CLC
LDLR
MERGE
b
siCtl
CLC
DiI-LDL
MERGE
siCLCa+b
CLC
DiI-LDL
MERGE

Fig.S4

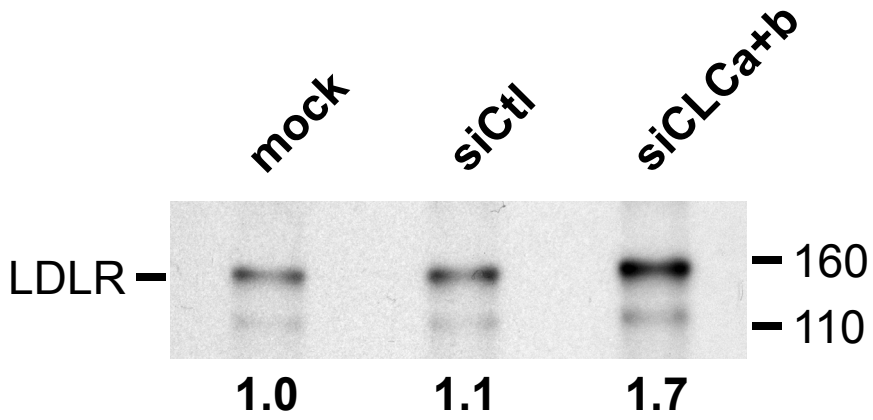

Fig.S5

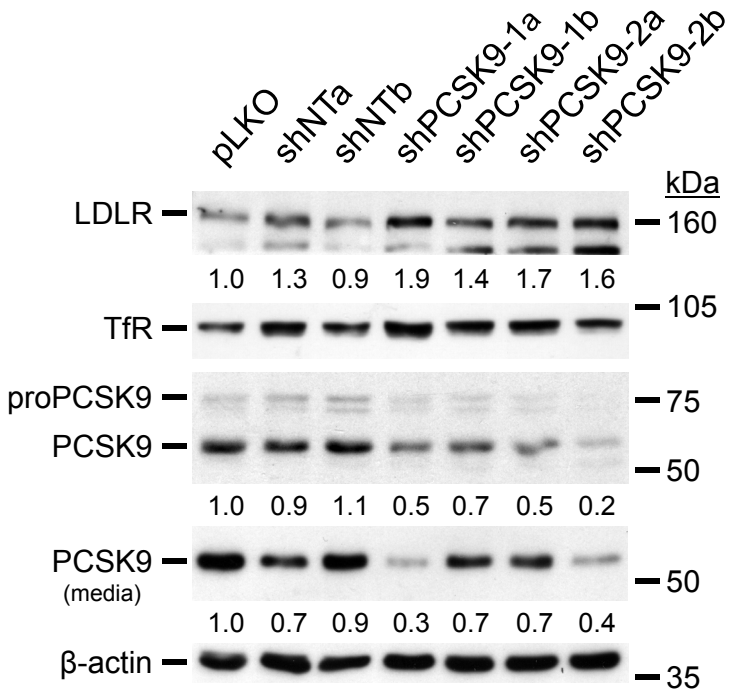
pLKO
shNTa
shNTb
shPCSK9-1a
shPCSK9-1b
shPCSK9-2a
shPCSK9-2b
kDa
LDLR
160
1.0 1.3 0.9 1.9 1.4 1.7 1.6
TfR
105
proPCSK9
PCSK9
75
50
1.0 0.9 1.1 0.5 0.7 0.5 0.2
PCSK9
(media)
50
1.0 0.7 0.9 0.3 0.7 0.7 0.4
β-actin
35

Fig.S6